

MODELLING THE POSTPEAK STRESS–DISPLACEMENT RELATIONSHIP OF CONCRETE IN UNIAXIAL COMPRESSION

TAKEAKI KOSHIKAWA*

*Hokkaido University
Faculty of Engineering
Kita 13, Nishi 8, Kita-ku, Sapporo 060-8628, Japan
e-mail: takeaki@eng.hokudai.ac.jp, www.hokudai.ac.jp

Key words: Uniaxial Compression, Postpeak, Localization, Fracture, Dissipated Energy, Concrete

Abstract. This paper presents a constitutive equation for the postpeak stress–displacement relationship of concrete in uniaxial compression. The relationship is modelled in relation to the process of postpeak energy dissipation increasing the postpeak displacement of the localized damage zone. The proposed equation includes three material parameters: compressive fracture energy, compressive strength, and critical postpeak displacement. The nondimensional form of the equation shows that a parameter determined from these three material parameters controls the shape of the postpeak stress–displacement curve. The predictions produced by the proposed equation are fit to uniaxial compression test results from concrete specimens with different slenderness ratios and strengths. The fitting results and experimental responses agree quite well.

1 INTRODUCTION

It is generally accepted that during the strain softening behaviour of concrete in its postpeak region under uniaxial compression, the damage is localized in certain zones and strain localization occurs [1]. Due to the localization phenomena, the postpeak portion of the stress–strain relationship is not a true material property, but is dependent on specimen size, with longer specimens exhibiting more brittle postpeak behaviour. Development of an appropriate postpeak relationship based on strain localization is important in accurately estimating the ductile capacity of concrete structures.

Published tests [1–3] have shown that the postpeak displacement of the localized damage zone is independent of specimen size. Some theoretical approaches have been proposed for analyzing the compressive behaviour of concrete based on this physical evidence. They in-

corporate a stress–strain relationship to describe the prepeak response and a stress–displacement relationship to describe postpeak behaviour as a material property [4–6]. These approaches can adequately predict concrete specimens' uniaxial compression test results, but the postpeak stress–displacement relationship is approximated by an overly simple equation. A more realistic equation for the postpeak stress–displacement relationship may be needed to further improve predictions.

The purpose of this paper is to develop a postpeak stress–displacement relationship for concrete in uniaxial compression. We propose a method to derive a realistic description based on the correlation between the postpeak stress–displacement relationship and the postpeak dissipated energy–displacement relationship. We present the nondimensional form of the proposed equation describing the postpeak stress–

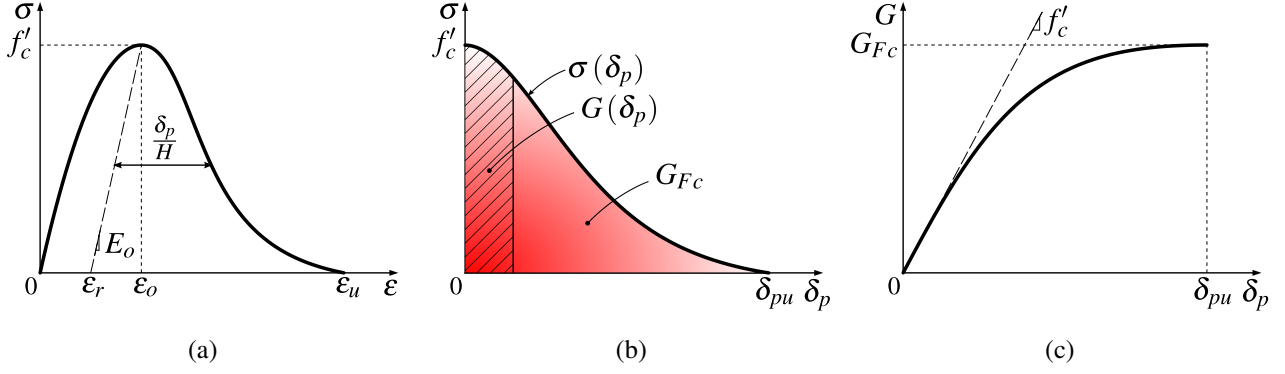


Figure 1: Correlation between (a) $\sigma - \varepsilon$ relationship, (b) $\sigma - \delta_p$ relationship and (c) $G - \delta_p$ relationship.

displacement relationship to show how the parameters influence the shape of the relationship. We use least squares fitting to uniaxial compression test results from concrete specimens with different slenderness ratios and strengths to estimate the material parameters used in the proposed equation, then compare the fitted results and experimental responses.

2 POSTPEAK STRESS–DISPLACEMENT RELATIONSHIP

2.1 Derivation of fundamental expression

We adopted the approach for the localized compression model proposed by Hillerborg [4] to model the postpeak stress–displacement relationship of concrete. Consider a one-dimensional concrete specimen under uniaxial compression. The specimen has a height of H , and a uniform cross-sectional area along the height. A typical stress–strain ($\sigma - \varepsilon$) relationship for a concrete specimen in compression as observed experimentally is illustrated in Figure 1(a). The relationship of the prepeak region up to the compressive strength f'_c can be considered to be approximately the same throughout the specimen. At the compressive strength, strain localization takes place, and strain softening begins in a localized damage zone.

In the postpeak region, the compressive behaviour of the whole specimen can be described as a combination of the behaviour inside and outside the damage zone. The postpeak displacement δ_p in the localized damage zone continues to increase, while the remainder of the

specimen unloads. Assuming that a linear unloading path from the compressive strength f'_c with slope E_o during unloading occurs outside the damage zone, the postpeak displacement δ_p shown in Figure 1(a) can be given by

$$\delta_p = \left(\varepsilon - \varepsilon_o + \frac{f'_c - \sigma}{E_o} \right) H \quad (1)$$

where ε and σ are the strain and stress, and ε_o is the strain corresponding to the compressive strength f'_c .

The progress of the postpeak displacement in the localized damage zone is accompanied by energy dissipation. The area under the curve of the postpeak stress–displacement ($\sigma - \delta_p$) relationship shown in Figure 1(b) corresponds to the amount of postpeak energy dissipated per unit specimen area [2, 7]. In this investigation, we assume that stress is a function of the postpeak displacement, i.e. $\sigma = \sigma(\delta_p)$ as shown in Figure 1(b), and the postpeak energy dissipated G is defined as

$$G = \int_0^{\delta_p} \sigma d\delta_p \quad (2)$$

where δ_p and σ are the postpeak displacement and stress at a given point on the curve of the relationship in Figure 1(b), respectively. The total postpeak energy dissipated by the time the postpeak displacement reaches the critical value δ_{pu} , corresponding to the stress condition $\sigma = 0$, can be defined as the compressive fracture energy G_{Fc} .

According to Equation (2), the postpeak dissipated energy is also assumed to be a function

of the postpeak displacement, i.e. $G = G(\delta_p)$, which satisfies the following equation.

$$\sigma = \frac{dG}{d\delta_p} \quad (3)$$

Equation (3) implies that the postpeak stress–displacement relationship can be defined by determining the postpeak dissipated energy–displacement ($G - \delta_p$) relationship with an appropriate equation and then differentiating that equation with respect to the postpeak displacement.

The essential features of the postpeak dissipated energy–displacement relationship shown in Figure 1(c) are the following:

1. The postpeak dissipated energy is an increasing function of the postpeak displacement, starting from $G = 0$ at $\delta_p = 0$ and increasing up to $G = G_{Fc}$ at $\delta_p = \delta_{pu}$.
2. The slope of the postpeak dissipated energy–displacement curve corresponds to the stress $\sigma = f'_c$ at $\delta_p = 0$ and $\sigma = 0$ at $\delta_p = \delta_{pu}$.

Taking these features into account, the postpeak dissipated energy–displacement relationship is assumed to be defined by the following proposed equation.

$$G = \frac{a_1\delta_p + a_2\delta_p^2}{1 + a_3\delta_p + a_4\delta_p^2} \quad (4)$$

where a_1 , a_2 , a_3 and a_4 are constants determined from the boundary conditions of the relationship. Considering an additional boundary condition, the horizontal tangent at the point of compressive strength on the postpeak stress–displacement curve, $d^2G/d\delta_p^2 = d\sigma/d\delta_p = 0$ at $\delta_p = 0$, together with the previously described boundary conditions of $G = 0$ and $\sigma = f'_c$ at $\delta_p = 0$, $G = G_{Fc}$ and $\sigma = 0$ at $\delta_p = \delta_{pu}$, the constants are given by

$$a_1 = f'_c$$

$$a_2 = f'_c \left(\frac{f'_c}{G_{Fc}} - \frac{2}{\delta_{pu}} \right)$$

$$a_3 = \frac{f'_c}{G_{Fc}} - \frac{2}{\delta_{pu}}$$

$$a_4 = \left(\frac{f'_c}{G_{Fc}} - \frac{1}{\delta_{pu}} \right)^2 \quad (5)$$

Thus, using Equations (3) to (5), the following expression can be derived.

$$\sigma = \frac{f'_c \left\{ 1 + 2 \left(\frac{f'_c}{G_{Fc}} - \frac{2}{\delta_{pu}} \right) \delta_p - \left(\frac{2f'_c}{G_{Fc}\delta_{pu}} - \frac{3}{\delta_{pu}^2} \right) \delta_p^2 \right\}}{\left\{ 1 + \left(\frac{f'_c}{G_{Fc}} - \frac{2}{\delta_{pu}} \right) \delta_p + \left(\frac{f'_c}{G_{Fc}} - \frac{1}{\delta_{pu}} \right)^2 \delta_p^2 \right\}^2} \quad (6)$$

As Equation (6) clearly shows, the shape of the postpeak stress–displacement curve in practical application depends on three material parameters: compressive fracture energy G_{Fc} , compressive strength f'_c , and critical postpeak displacement δ_{pu} .

2.2 Nondimensional form expression

To demonstrate the shape of the postpeak stress–displacement relationship obtained using Equation (6), we introduce the following new parameter A_p , determined using those three material parameters.

$$A_p = \frac{G_{Fc}}{f'_c\delta_{pu}} \quad (7)$$

As can be seen from Figure 1(b) and Equation (7), the parameter A_p represents the ratio between the area under the curve of the postpeak stress–displacement relationship and the area of a rectangle given by f'_c times δ_{pu} . Considering softening behaviour, the parameter A_p must be a positive value less than 1.

Using the parameter A_p , Equation (6) can be rewritten in the following nondimensional form.

$$\frac{\sigma}{f'_c} = \frac{1 + 2 \left(\frac{1}{A_p} - 2 \right) \frac{\delta_p}{\delta_{pu}} - \left(\frac{2}{A_p} - 3 \right) \left(\frac{\delta_p}{\delta_{pu}} \right)^2}{\left\{ 1 + \left(\frac{1}{A_p} - 2 \right) \frac{\delta_p}{\delta_{pu}} + \left(\frac{1}{A_p} - 1 \right)^2 \left(\frac{\delta_p}{\delta_{pu}} \right)^2 \right\}^2} \quad (8)$$

In this expression, stress and postpeak displacement are reduced to nondimensional forms by dividing them by compressive strength f'_c and critical postpeak displacement δ_{pu} , respectively. The parameter A_p thus becomes a single parameter that determines the relationship. Figure 2 shows the nondimensional form of the postpeak stress–displacement relationship with various values of A_p . The value of A_p influences the shape of the relationship, with larger values exhibiting more ductile postpeak behaviour. Based on Figure 2, it seems appropriate for parameter A_p to be less than 0.5 for realistic representation of the behaviour of plain concrete.

Another possible expression of the nondimensional form of Equation (6) that makes use of parameter A_p is given by

$$\frac{\sigma}{f'_c} = \frac{1 + 2(1 - 2A_p) \frac{f'_c \delta_p}{G_{Fc}} - (2 - 3A_p) A_p \left(\frac{f'_c \delta_p}{G_{Fc}} \right)^2}{\left\{ 1 + (1 - 2A_p) \frac{f'_c \delta_p}{G_{Fc}} + (1 - A_p)^2 \left(\frac{f'_c \delta_p}{G_{Fc}} \right)^2 \right\}^2} \quad (9)$$

In this expression, G_{Fc}/f'_c is used to reduce the postpeak displacement to a nondimensional form.

As a special case, if $A_p = 0$ is used and the value of the critical postpeak displacement δ_{pu} is assumed to be infinity, Equation (9) can be rewritten in the following simple form

$$\frac{\sigma}{f'_c} = \frac{1 + 2 \frac{f'_c \delta_p}{G_{Fc}}}{\left\{ 1 + \frac{f'_c \delta_p}{G_{Fc}} + \left(\frac{f'_c \delta_p}{G_{Fc}} \right)^2 \right\}^2} \quad (10)$$

If $A_p = 1$ is used, Equation (9) (or (8)) becomes

$$\frac{\sigma}{f'_c} = 1 \quad (11)$$

These two special cases are illustrated in Figure 3.

3 FITTING TO EXPERIMENTAL RESULTS

In the postpeak stress–displacement relationship proposed in the previous section there are

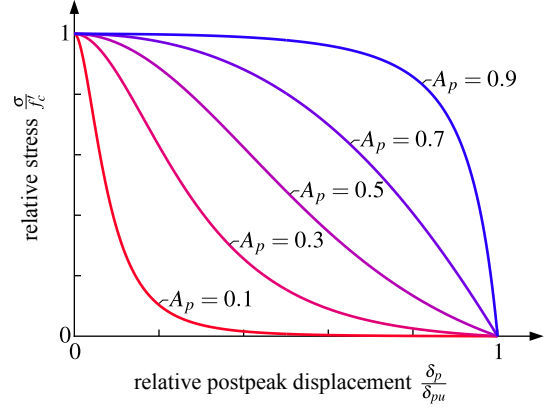


Figure 2: Nondimensional form of postpeak stress–displacement relationship with various parameters A_p .

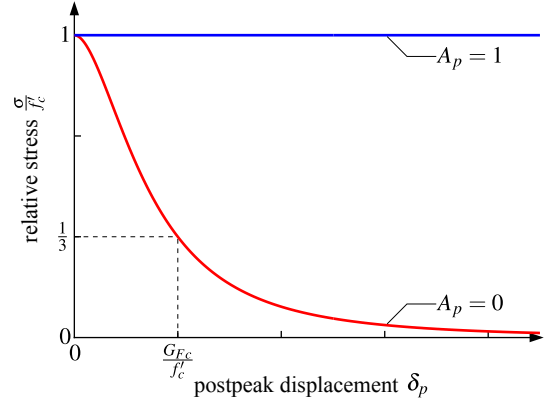


Figure 3: Postpeak stress–displacement relationship with parameters $A_p = 0$ and 1.

three material parameters, G_{Fc} , f'_c and δ_{pu} (or A_p), that need to be determined for practical applications. While the compressive strength f'_c is easy to determine experimentally, the compressive fracture energy G_{Fc} and critical postpeak displacement δ_{pu} are hard to measure using uniaxial compression tests because the tests generally cannot continue to the point where the stress drops to zero. However by fitting the proposed relationship to experimental data obtained through the point where the stress drops to a certain postpeak level, these material parameters can be estimated. In this investigation, we conducted uniaxial compression tests on concrete specimens, and then fitted the postpeak stress–displacement relationship using least squares to estimate the material parameters of each concrete specimen.

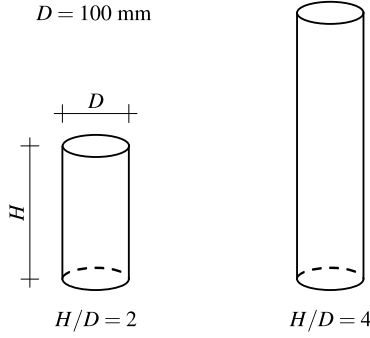


Figure 4: Concrete specimens with different heights.

3.1 Uniaxial compression test

In the uniaxial compression test, specimens with different slenderness ratios and strengths were tested. As shown in Figure 4 and Table 1, we used two sets of cylindrical specimens with the same diameters $D = 100$ mm and heights $H = 200$ mm and 400 mm, prepared with two concrete mixes. To prevent the effect of bleeding in concrete, the specimens were cast 200 mm taller than their proper heights, and 100 mm was cut from the top and bottom of each specimen. At the time of loading, friction reducing pads consisting of two 0.05 mm thick Teflon sheets with silicon grease were placed between the specimen and the loading platens. The uniaxial compression test results showing compressive strength f'_c , strain at compressive strength ε_o and the modulus of elasticity E_c are given in Table 2. The compressive strengths were about 25 N/mm² and 50 N/mm² for the Mix I and II concretes, respectively.

3.2 Fitting result

The postpeak stress–displacement relationship was fitted to the experimental results using Equation (9). The postpeak displacement δ_p of the test results was calculated by Equation (1), assuming that the slope E_o is equal to the modulus of elasticity E_c . The compressive fracture energy G_{Fc} was assumed to be the coefficient estimated from the least squares fitting procedure. By setting parameter A_p to various values less than 0.5, corresponding values of compressive fracture energy G_{Fc} were obtained

Table 1: Mix proportions

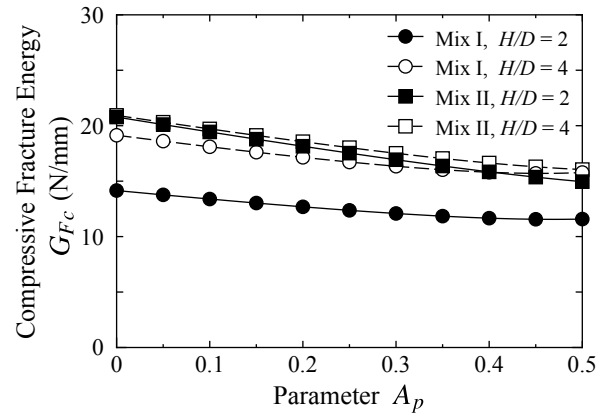
Mix	W/C (%)	s/a (%)	Unit weight (kg/m ³)				Ad (C×%)
			W	C	S	G	
I	56.2	44.5	179	318	784	998	0.006*
II	32.0	47.2	175	547	747	853	0.006* 1.1**

* air entraining agent

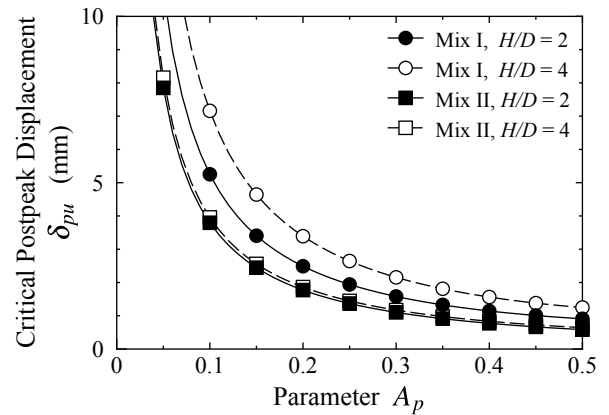
** air entraining and high-range water reducing agent

Table 2: Specimens and test results

Mix	H/D	H (mm)	f'_c (N/mm ²)	ε_o ($\times 10^{-6}$)	E_c (kN/mm ²)
I	4	400	25.3	1805	22.5
II	2	200	51.2	2875	26.4
II	4	400	49.8	2607	25.2

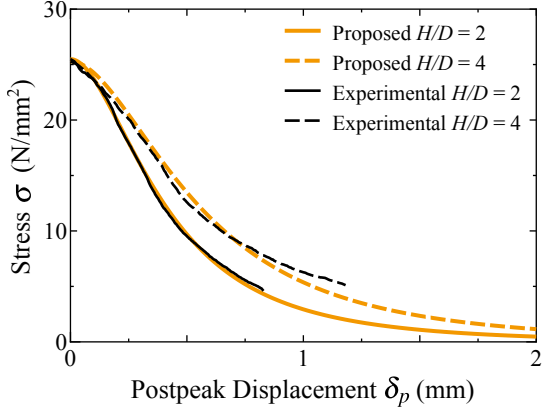


(a) Compressive fracture energy G_{Fc}

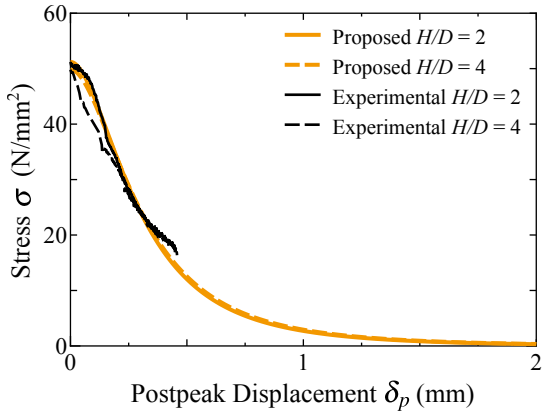


(b) Critical postpeak displacement δ_{pu}

Figure 5: Fitting results for various parameters A_p .



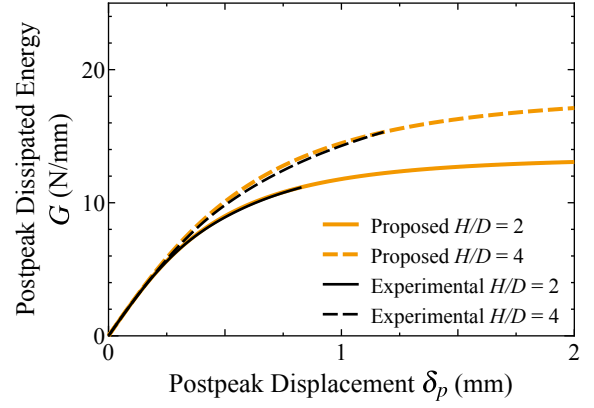
(a) Mix I



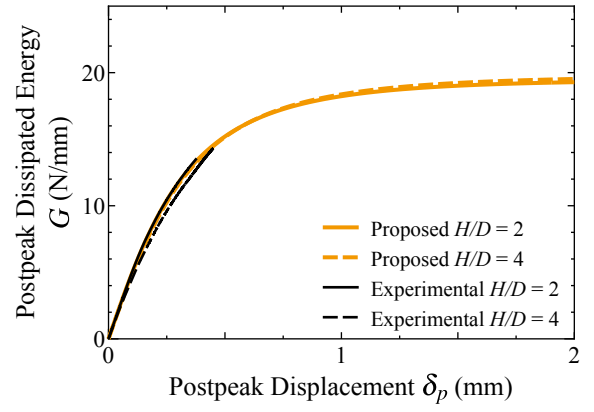
(b) Mix II

Figure 6: Experimental and proposed $\sigma - \delta_p$ relationships (using $A_p = 0.1$).

for all the specimens as shown in Figure 5(a). Also, the values of critical postpeak displacement δ_{pu} calculated using Equation (7) are shown in Figure 5(b). As can be readily seen from Figure 5, for all specimens, the variation of estimated values of G_{Fc} or δ_{pu} compared to the values of A_p show the same tendency although each specimen's values are different. Since the values of G_{Fc} decrease only slightly as the values of A_p increase, they can be thought to be generally consistent in this range of A_p . On the contrary, the corresponding values of δ_{pu} are significantly affected by the values of A_p . We could not measure the actual values of δ_{pu} in this test, but according to the fitting results, we assumed them to be at least greater than 1 mm. As an example, we present a comparison between the resulting postpeak stress–



(a) Mix I

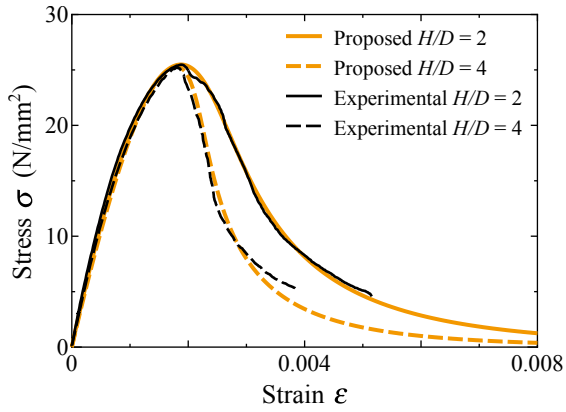


(b) Mix II

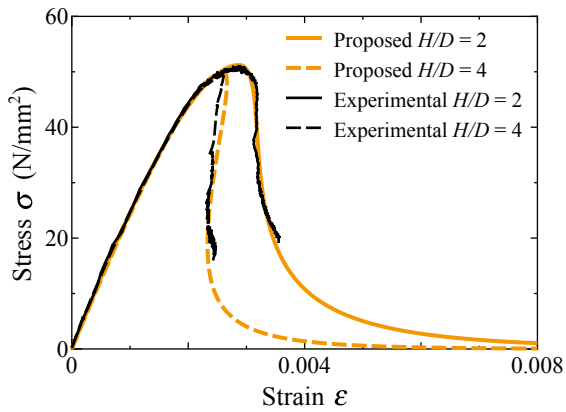
Figure 7: Experimental and proposed $G - \delta_p$ relationships (using $A_p = 0.1$).

displacement relationships using $A_p = 0.1$ and the experimental results in Figure 6. Overall, the proposed relationship is quite consistent with the the experimental results.

Another set of comparisons of the fitting results using $A_p = 0.1$ against the experimental results are shown in Figures 7 and 8 for the postpeak dissipated energy–displacement relationship and the stress–strain relationship, respectively. The postpeak dissipated energy G of the test results was obtained from the area under the curve of the postpeak stress–displacement relationship calculated by the trapezoidal rule. The strain ε of the postpeak region based on the proposed relationship was calculated using Equation (1). For the prepeak region, we used the following equation [8] with the parameter values listed in Table 2.



(a) Mix I



(b) Mix II

 Figure 8: Experimental and proposed σ - ε relationships (using $A_p = 0.1$).

$$\frac{\sigma}{f'_c} = \frac{\frac{E_c \varepsilon_o}{f'_c} \frac{\varepsilon}{\varepsilon_o} - \left(\frac{\varepsilon}{\varepsilon_o}\right)^2}{1 + \left(\frac{E_c \varepsilon_o}{f'_c} - 2\right) \frac{\varepsilon}{\varepsilon_o}} \quad (12)$$

The results of these figures, including Figure 6 indicate that the proposed approach for modelling the postpeak behaviour of concrete based on the correlation of these relationships is valid.

4 CONCLUSIONS

We have presented a constitutive equation for the postpeak stress–displacement relationship of concrete in uniaxial compression. The derivation of the equation is based on the correlation between this relationship and the postpeak dissipated energy–displacement relationship. The proposed equation includes three material parameters: compressive fracture energy,

compressive strength, and critical postpeak displacement at the point when the stress drops to zero. The nondimensional form of the equation shows that the parameter A_p , determined from those three material parameters, controls the shape of the postpeak stress–displacement curve. For realistic representation of postpeak behaviour in plain concrete, values of parameter A_p that are less than 0.5 seem appropriate.

The results of least squares fitting of the equation to uniaxial compression tests of concrete specimens with different slenderness ratios and strengths show that the value of parameter A_p has more effect on the estimated value of the critical postpeak displacement than does the compressive fracture energy. For any specimen, the fitted results using $A_p = 0.1$ and the experimental responses agree quite well with respect to the stress–strain relationship, the postpeak stress–displacement relationship and the postpeak dissipated energy–displacement relationship.

REFERENCES

- [1] Van Mier, J.G.M., 1986. Multiaxial strain-softening of concrete, Part I: Fracture, Part II: Load-Histories. *Mater. Struct.* **19**:179–200.
- [2] Jansen, D.C. and Shah, S.P., 1997. Effect of length on compressive strain softening of concrete. *J. Engrg. Mech.* **123**:25–35.
- [3] Van Mier, J.G.M., Shah, S.P., Arnaud, M. et al., 1997. Strain-softening of concrete in uniaxial compression. *Mater. Struct.* **30**:195–209.
- [4] Hillerborg, A., 1990. Fracture mechanics concepts applied to moment capacity and rotational capacity of reinforced concrete beams. *Engrg. Fract. Mech.* **35**:233–240.
- [5] Fantilli, A.P., Mihashi, H. and Vallini, P., 2007. Post-peak behavior of cement-based materials in compression. *ACI Mat. J.* **104**:501–510.

- [6] Carpinteri, A., Corrado, M., Mancini, G. and Paggi, M., 2009. The overlapping crack model for uniaxial and eccentric concrete compression tests. *Mag. Conc. Res.* **61**:745–757.
- [7] Vonk, R.A., 1993. A micromechanical investigation of softening of concrete loaded in compression. *Heron*, **38**:1–94.
- [8] CEB (Comité Euro-International du Béton), 1990. CEB-FIP Model Code 1990. *Bulletin d'Information*, **195**, CEB